J|A|C|S ARTICLES

Published on Web 07/15/2009

Viral Capsid DNA Aptamer Conjugates as Multivalent Cell-Targeting Vehicles

Gary J. Tong, Sonny C. Hsiao, Zachary M. Carrico, and Matthew B. Francis*

Department of Chemistry, University of California, Berkeley, and Materials Sciences Division, Lawrence Berkeley National Laboratories, Berkeley, California 94720-1460

Received May 12, 2009; E-mail: francis@cchem.berkeley.edu

Abstract: Nucleic acid aptamers offer significant potential as convenient and evolvable targeting groups for drug delivery. To attach them to the surface of a genome-free viral capsid carrier, an efficient oxidative coupling strategy has been developed. The method involves the periodate-mediated reaction of phenylene diamine substituted oligonucleotides with aniline groups installed on the outer surface of the capsid shells. Up to 60 DNA strands can be attached to each viral capsid with no apparent loss of base-pairing capabilities or protein stability. The ability of the capsids to bind specific cellular targets was demonstrated through the attachment of a 41-nucleotide sequence that targets a tyrosine kinase receptor on Jurkat T cells. After the installation of a fluorescent dye on the capsid interior, capsids bearing the cell-targeting sequence showed significant levels of binding to the cells relative to those of control samples. Colocalization experiments using confocal microscopy indicated that the capsids were endocytosed and trafficked to lysosomes for degradation. These observations suggest that aptamer-labeled capsids could be used for the targeted drug delivery of acid-labile prodrugs that would be preferentially released upon lysosomal acidification.

Introduction

Multivalent and targeted delivery vehicles offer great promise for drug administration and diagnostic imaging. A number of core scaffolds, including polymers,[1−3] dendrimers,[4,5] inorganic nanoparticles,[6−8] and liposomes,[9,10] have been used with considerable success in these applications. In terms of biomolecule-based vectors, engineered heat shock cages[11] and viral capsids[12] have also been developed to house drug molecules on their interior. For each of these carrier types, a critically important consideration is the installation of receptor-binding groups that enable the selective association of the carriers with targeted tissue types. The most common molecular strategies for this purpose have involved folic acid,[13,14] cobalamin,[15,16] carbohydrates,[17] peptides and antibodies,[18,19] and nucleic acid aptamers.[20] The rich chemical diversity of these molecules, added to the desire to attach multiple copies of each to scaffolds of varying composition, calls for chemical reactions that are exquisitely functional-group-tolerant and proceed under physiological conditions.

An increasing number of chemoselective coupling reactions have been advanced for the labeling of full-sized biomolecules.[21−25] All of the reported methods have their particular strengths and ideal usages, and with the addition of each technique, new possibilities have arisen for the generation of complex structures comprising multiple biomolecular components. To add to this list, we have reported a highly efficient oxidative coupling reaction that occurs between anilines and phenylene diamines in the presence of aqueous sodium perio-

(1) Liu, S.; Maheshwari, R.; Kiick, K. L. *Macromolecules* **2009**, *42*, 3–13.
(2) Farokhzad, O. C.; Cheng, J.; Teply, B. A.; Sherifi, I.; Jon, S.; Kantoff, P. W.; Richie, J. P.; Langer, R. *Proc. Natl. Acad. Sci.* **2006**, *103*, 6315–6320.
(3) Dhar, S.; Gu, F. X.; Langer, R.; Farokhzad, O. C.; Lippard, S. J. *Proc. Natl. Acad. Sci.* **2008**, *105*, 17356–17361.
(4) Lee, C. C.; MacKay, J. A.; Frechet, J. M. J.; Szoka, F. C. *Nat. Biotechnol.* **2005**, *23*, 1517–1526.
(5) Almutairi, A.; Rossin, R.; Shokeen, M.; Hagooly, A.; Ananth, A.; Capoccia, B.; Guillaudeu, S.; Abendschein, D.; Anderson, C. J.; Welch, M. J.; Fréchet, J. M. J. *Proc. Natl. Acad. Sci.* **2009**, *106*, 685–690.
(6) Liong, M.; Lu, J.; Kovochich, M.; Xia, T.; Ruehm, S. G.; Nel, A. E.; Tamanoi, F.; Zink, J. I. *ACS Nano* **2008**, *2*, 889–896.
(7) Medarova, Z.; Pham, W.; Farrar, C.; Petkova, V.; Moore, A. *Nat. Med.* **2007**, *13*, 372–377.
(8) Javier, D. J.; Nitin, N.; Levy, M.; Ellington, A.; Richards-Kortum, R. *Bioconjugate Chem.* **2008**, *19*, 1309–1312.
(9) Lee, R.; Low, P. *J. Biol. Chem.* **1994**, *269*, 3198–3204.
(10) Medinai, O. P.; Zhu, Y.; Kairemo, K. *Curr. Pharm. Des.* **2004**, *10*, 2981–2989.
(11) Flenniken, M. L.; Willits, D. A.; Harmsen, A. L.; Liepold, L. O.; Harmsen, A. G.; Young, M. J.; Douglas, T. *Chem. Biol.* **2006**, *13*, 161–170.
(12) Flenniken, M.; Uchida, M.; Liepold, L.; Kang, S.; Young, M.; Douglas, T. *Viruses Nanotechnol.* **2009**, *327*, 71–93.
(13) Hilgenbrink, A. R.; Low, P. S. *J. Pharm. Sci.* **2005**, *94*, 2135–2146.
(14) Sudimack, J.; Lee, R. J. *Adv. Drug Delivery Rev.* **2000**, *41*, 147–162.
(15) Gupta, Y.; Kohli, D.; Jain, S. *Crit. Rev. Therap. Drug Carrier Syst.* **2008**, *25*, 347–379.
(16) Petrus, A.; Fairchild, T.; Doyle, R. *Angew. Chem., Int. Ed.* **2009**, *48*, 1022–1028.
(17) Darbre, T.; Reymond, J. *Curr. Top. Med. Chem.* **2008**, *8*, 1286–93.
(18) Brown, K. C. *Curr. Opin. Chem. Biol.* **2000**, *4*, 16–21.
(19) Schrama, D.; Reisfeld, R. A.; Becker, J. C. *Nat. Rev. Drug Discov.* **2006**, *5*, 147–159.
(20) Lee, J. F.; Stovall, G. M.; Ellington, A. D. *Curr. Opin. Chem. Biol.* **2006**, *10*, 282–289.
(21) Kolb, H. C.; Finn, M. G.; Sharpless, K. B. *Angew. Chem., Int. Ed.* **2001**, *40*, 2004–2021.
(22) Baskin, J. M.; Prescher, J. A.; Laughlin, S. T.; Agard, N. J.; Chang, P. V.; Miller, I. A.; Lo, A.; Codelli, J. A.; Bertozzi, C. R. *Proc. Natl. Acad. Sci. U.S.A.* **2007**, *104*, 16793–16797.
(23) Jencks, W. P. *J. Am. Chem. Soc.* **1959**, *81*, 475–481.
(24) Wang, Q.; Chan, T. R.; Hilgraf, R.; Fokin, V. V.; Sharpless, K. B.; Finn, M. G. *J. Am. Chem. Soc.* **2003**, *125*, 3192–3193.
(25) Saxon, E.; Bertozzi, C. R. *Science* **2000**, *287*, 2007–2010.

10.1021/ja903857f CCC: $40.75

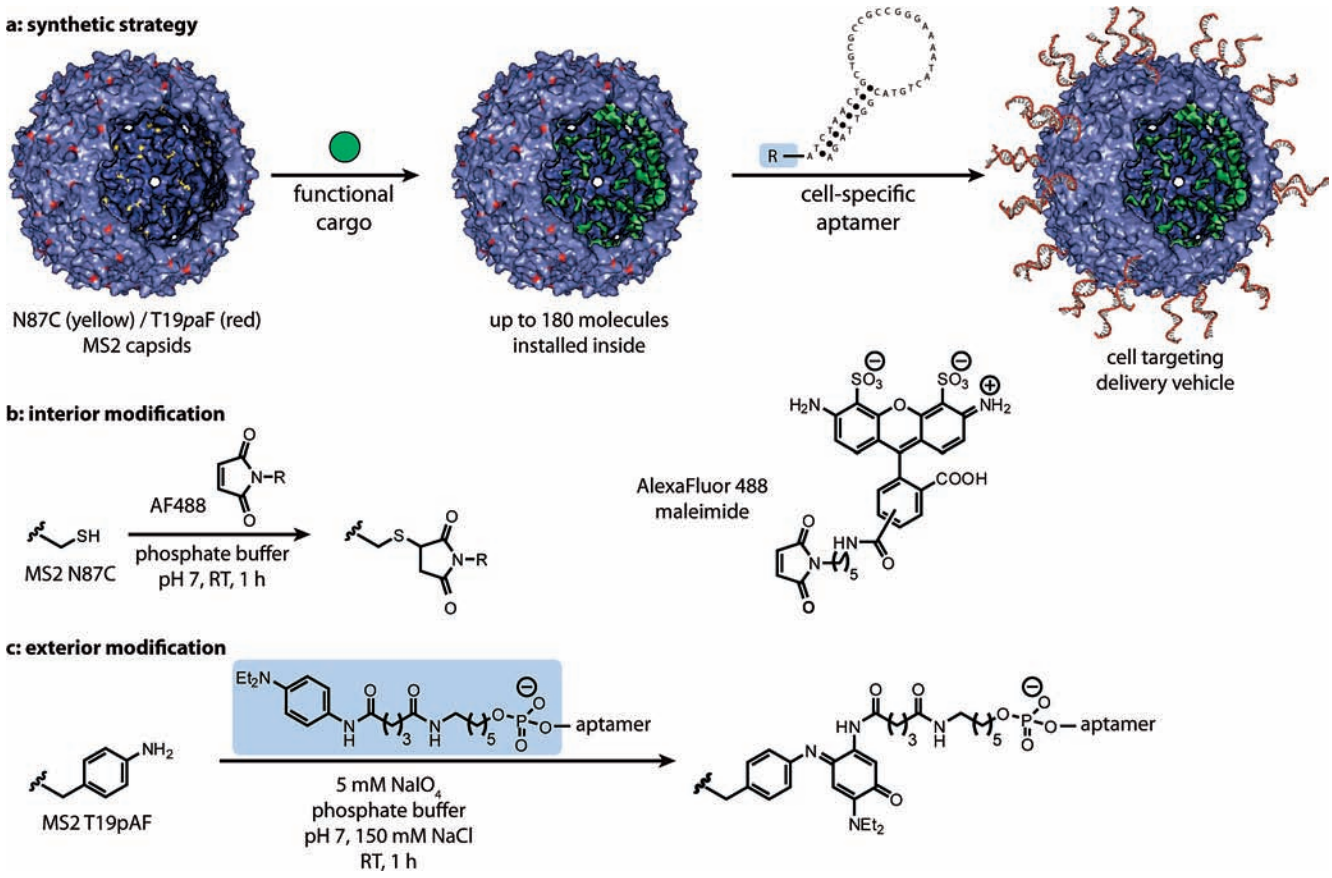

Figure 1. Dual-surface modification of capsids for targeted delivery. The overall synthetic strategy is shown in (a). (b) For interior surface modification, an N87C mutation on the MS2 coat protein allows for site-specific alkylation. Up to 180 cargo molecules can be installed in these locations. (c) For exterior surface modification, the aptamer is first modified with a phenylene diamine group. A T19*p*aF mutation on the capsid allows for the attachment of the modified DNA to the exterior surface of MS2 by a $NaIO_4$-mediated oxidative coupling reaction.

date.[26] This reaction has shown exceptional chemoselectivity to date and proceeds rapidly at micromolar concentrations and at neutral pH. In this report, we apply this method to attach 20−60 copies of a DNA aptamer to the surface of genome-free viral capsids, as outlined in Figure 1a. The resulting multivalent assemblies bind to tyrosine kinase receptors on the surface of Jurkat cells and are readily endocytosed. Finally, we show that this chemistry can be combined with other bioconjugation methods that could install functional drug molecules within the carriers. The ability of the oxidative coupling strategy to prepare these heterobiomolecular structures bodes well for its use in the preparation of many different types of delivery vehicles.

Results and Discussion

Bacteriophage MS2 provides a readily available scaffold for the construction of targeted delivery agents. The protein coat of this virus consists of 180 sequence-identical monomers that are arranged in a hollow spherical structure.[27,28] The coat protein monomer can be expressed and self-assembled readily in *Escherichia coli*, yielding robust, nontoxic, and biodegradable structures that are genome-free.[29] As MS2 capsids possess 32 pores that allow access to the inside of the capsid, selective modification can be achieved on both the interior and the exterior surfaces using orthogonal bioconjugation reactions.[30,31] In previous reports, we have shown that tyrosine-based chemistry can be used to install F-18 positron emission tomography tracers[32] and Gd-based magnetic resonance imaging contrast enhancement agents[33,34] to allow their use in imaging applications.

To endow the capsids with specific targeting capabilities, we have developed an efficient synthetic method to attach nucleic acid aptamers to their surfaces.[35] With the development of the SELEX (systematic evolution of ligands by exponential enrichment) process, aptamer sequences can be evolved to bind virtually any target,[36,37] and once the composition has been identified, they can be obtained readily using automated solid-

(26) Hooker, J. M.; Esser-Kahn, A. P.; Francis, M. B. *J. Am. Chem. Soc.* **2006**, *128*, 15558–15559.
(27) Valegard, K.; Liljas, L.; Fridborg, K.; Unge, T. *Nature* **1990**, *345*, 36–41.
(28) Mastico, R. A.; Talbot, S. J.; Stockley, P. G. *J. Gen. Virol.* **1993**, *74*, 541–548.
(29) Carrico, Z. M.; Romanini, D. W.; Mehl, R. A.; Francis, M. B. *Chem. Commun.* **2008**, 1205–1207.
(30) Hooker, J. M.; Kovacs, E. W.; Francis, M. B. *J. Am. Chem. Soc.* **2004**, *126*, 3718–3719.
(31) Kovacs, E. W.; Hooker, J. M.; Romanini, D. W.; Holder, P. G.; Berry, K. E.; Francis, M. B. *Bioconjugate Chem.* **2007**, *18*, 1140–1147.
(32) Hooker, J. M.; O'Neil, J. P.; Romanini, D. W.; Taylor, S. E.; Francis, M. *Mol. Imag. Biol.* **2008**, *10*, 182–191.
(33) Hooker, J. M.; Datta, A.; Botta, M.; Raymond, K. N.; Francis, M. B. *Nano Lett.* **2007**, *7*, 2207–2210.
(34) Datta, A.; Hooker, J. M.; Botta, M.; Francis, M. B.; Aime, S.; Raymond, K. N. *J. Am. Chem. Soc.* **2008**, *130*, 2546–2552.
(35) For an alternative approach for the attachment of DNA strands to the cowpea mosaic virus, see Strable, E.; Johnson, J. E.; Finn, M. G. *Nano Lett.* **2004**, *4*, 1385−1389.
(36) Ellington, A. D.; Szostak, J. W. *Nature* **1990**, *346*, 818–822.

phase synthesis techniques. Their synthesis is also amenable to the introduction of modified backbones that can improve stability[38,39] or impart novel functionality.[40] In addition, aptamers can often match or even surpass the specificity and affinity of antibodies, with the added convenience of smaller size. These qualities make them attractive tools for the development of targeted therapeutics and imaging platforms with widely varied targeting capabilities. This potential has been realized in a number of recent reports.[41−50]

To install oligonucleotide aptamers on the surface of the MS2 capsids, we chose a previously reported $NaIO_4$-mediated oxidative coupling strategy.[26,51] This method entails the chemoselective coupling of an *N*,*N*-diethyl-*N*′-acylphenylene diamine moiety (Figure 1c) to an aniline in the presence of $NaIO_4$. In previous studies, sodium periodate was used to oxidize the 1,2-diol at the 3′-end of RNA to introduce aldehyde functionalities, but was not observed to degrade the RNA strand.[52] Although this observation suggests that RNA-based aptamers could be used with our method, we chose to proceed with DNA because of its enhanced stability toward hydrolysis during the isolation and handling steps.

The aniline coupling partners can be introduced on the exterior surface of MS2 capsids either through direct chemical modification[26] or through the introduction of an unnatural amino acid, *p*-aminophenylalanine (*p*aF), into position 19 of the MS2 coat protein using the amber stop codon suppression system.[29,53] Using the latter route, we reported previously that the oxidative coupling strategy can introduce over 100 copies of peptide chains bearing phenylene diamine groups. For this report, we again used the suppression method to produce capsids bearing the T19*p*aF mutation (MS2-*p*aF19), thus providing 180 aniline groups for coupling to the exterior surface. In this case, however, we also introduced an N87C mutation to provide 180 sulfhydryl groups on the interior surface for cargo installation (Figure 1b).

Table 1. DNA Sequences Used for Attachment to MS2 Capsids[a]

strand	sequence
A	5′-TCATACGACTCACTCTAGGGA-3′
B	5′-ATCTAACTGCTGCGCCGCCGGG AAAATACTGTACGGTTAGA-3′
C	5′-CCCTAGAGTGAGTCGTATGACC CTAGAGTGAGTCGTATGAA-3′

[a] All sequences have the phenylene diamine moiety attached through an amino group at the 5′ terminus (see Figure 1c).

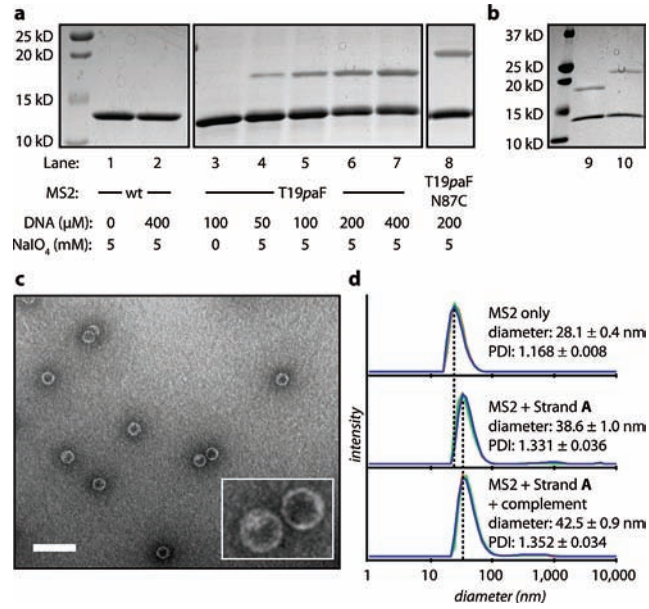

Figure 2. Analysis of DNA attachment to the exterior surface of MS2. (a) MS2-DNA conjugates were analyzed by SDS-PAGE followed by Coomassie staining. Lanes 1−7 were reacted with strand **A**. Lane 8 shows the reaction with strand **B**. (b) A gel-shift assay confirmed DNA competency for base pairing after conjugation to MS2. Lane 10 includes the complementary sequence to strand **A** with an additional 20 adenine bases for an increased eletrophoretic shift, whereas lane 9 has no additional DNA added. Transmission electron micrograph images (c) and dynamic light scattering analysis (d) showed intact capsids after DNA conjugation. In addition, DLS showed a significant increase in the diameter upon conjugation of strand **A**, as well as an additional increase in diameter upon addition of the 20-base complementary sequence to strand **A** (without the additional 20-base overhang). The scale bar in the TEM image represents 100 nm.

The resulting MS2-*p*aF19-N87C double mutant was obtained with a yield of 10 mg/L of culture.

To develop the reaction conditions, a 20-base DNA sequence, strand **A** (Table 1), was first selected. Starting from an amine-terminated version of this sequence, the *N*,*N*-diethyl-*N*′-acylphenylene diamine moiety was introduced through acylation with an *N*-hydroxysuccinimide-ester containing precursor. Next, reaction conditions were screened by varying the concentrations of reacting DNA, sodium periodate, and reaction time. Upon analysis by SDS-PAGE, the DNA conjugates exhibited a significant gel shift relative to the unmodified monomers (Figure 2a), allowing facile quantification of the reaction conversion using densitometry after Coomassie staining. Optimal DNA coupling was achieved using 10−20 equiv (200−400 μM) of the DNA conjugate relative to MS2-*p*aF19 coat protein (20 μM, based on monomer) and 250 equiv of periodate (5 mM) at room temperature for 1 h. An additional increase in the coupling efficiency was observed when the reaction was run at higher concentrations of sodium chloride, which is likely due to the ability of the higher ionic strength to shield the buildup of negative charge density on the capsid surface as more DNA is

(37) Tuerk, C.; Gold, L. *Science* **1990**, *249*, 505–510.
(38) Keefe, A. D.; Cload, S. T. *Curr. Opin. Chem. Biol.* **2008**, *12*, 448–456.
(39) Eulberg, D.; Klussmann, S. *ChemBioChem* **2003**, *4*, 979–983.
(40) Li, M.; Lin, N.; Huang, Z.; Du, L.; Altier, C.; Fang, H.; Wang, B. *J. Am. Chem. Soc.* **2008**, *130*, 12636–12638.
(41) Farokhzad, O. C.; Jon, S.; Khademhosseini, A.; Tran, T. T.; LaVan, D. A.; Langer, R. *Cancer Res.* **2004**, *64*, 7668–7672.
(42) Nimjee, S. M.; Rusconi, C. P.; Sullenger, B. A. *Annu. Rev. Med.* **2005**, *56*, 555–583.
(43) McNamara, J. O.; Andrechek, E. R.; Wang, Y.; Viles, K. D.; Rempel, R. E.; Gilboa, E.; Sullenger, B. A.; Giangrande, P. H. *Nat. Biotechnol.* **2006**, *24*, 1005–1015.
(44) Bagalkot, V.; Farokhzad, O. C.; Langer, R.; Jon, S. *Angew. Chem., Int. Ed.* **2006**, *45*, 8149–8152.
(45) Bagalkot, V.; Zhang, L.; Levy-Nissenbaum, E.; Jon, S.; Kantoff, P. W.; Langer, R.; Farokhzad, O. C. *Nano Lett.* **2007**, *7*, 3065–3070.
(46) Chu, T. C.; Marks, J. W.; Lavery, L. A.; Faulkner, S.; Rosenblum, M. G.; Ellington, A. D.; Levy, M. *Cancer Res.* **2006**, *66*, 5989–5992.
(47) Chu, T. C.; Twu, K. Y.; Ellington, A. D.; Levy, M. *Nucleic Acids Res.* **2006**, *34*, e73.
(48) Hicke, B. J.; Stephens, A. W.; Gould, T.; Chang, Y.; Lynott, C. K.; Heil, J.; Borkowski, S.; Hilger, C.; Cook, G.; Warren, S.; Schmidt, P. G. *J. Nucl. Med.* **2006**, *47*, 668–678.
(49) Bunka, D. H. J.; Stockley, P. G. *Nat. Rev. Micro.* **2006**, *4*, 588–596.
(50) Huang, Y.; Shangguan, D.; Liu, H.; Phillips, J. A.; Zhang, X.; Chen, Y.; Tan, W. *ChemBioChem* **2009**, *10*, 862–868.
(51) For an additional example of aromatic amino acid activation using periodate, see Liu, B.; Burdine, L.; Kodadek, T. *J. Am. Chem. Soc.* **2006**, *128*, 15228−15235.
(52) Wu, T. P.; Ruan, K. C.; Liu, W. Y. *Nucleic Acids Res.* **1996**, *24*, 3472–3473.
(53) Mehl, R. A.; Anderson, J. C.; Santoro, S. W.; Wang, L.; Martin, A. B.; King, D. S.; Horn, D. M.; Schultz, P. G. *J. Am. Chem. Soc.* **2003**, *125*, 935–939.

attached (see Figure S1 in the Supporting Information). For strand **A**, SDS-PAGE and Coomassie staining, followed by optical densitometry, indicated that 32% of the capsid monomers had been modified with a single strand of DNA. As there are 180 monomers in each capsid, this corresponds to 55 DNA strands on the surface of each. Longer sequences showed slightly lower conversion, most likely due to increased steric effects as well as electrostatic repulsion.

Following the reaction, the modified capsids could be separated from excess DNA using either size exclusion chromatography or centrifugal concentrators with 100 kDa molecular weight cutoffs. As a technical note, care must be taken to remove all glycerol, ethylene glycol, or other vicinal diols from the samples to prevent them from reacting with the periodate.

As shown in Figure 2c,d, the resulting capsids remained intact by transmission electron microscopy (TEM) and dynamic light scattering (DLS). DLS showed an increase of 10.5 ± 0.7 nm in the hydrodynamic diameter upon conjugation of strand **A** to the capsids. When the complementary strand was introduced, the diameter increased by an additional 3.9 ± 1.0 nm, suggesting that the DNA was still capable of Watson−Crick−Franklin base pairing when conjugated to the exterior of the capsid. The ability to base pair also provides good evidence that the DNA strands are stable throughout the oxidative coupling conditions. Base pairing of the conjugated DNA was further confirmed on denatured capsid monomers by SDS-PAGE using a gel-shift assay (Figure 2b).

For functionalization of the interior surface of MS2, standard cysteine bioconjugation was chosen. MS2 contains two native cysteines that have proven to be inaccessible under normal maleimide bioconjugation conditions. Therefore, a double mutant (MS2-*p*aF19-N87C) was expressed to introduce a cysteine on the interior surface. The reactivity of the cysteine mutant is shown in Figure S2 in the Supporting Information, where MS2 becomes fluorescently labeled in the presence of Alexa Fluor 488 maleimide (AF488). For this sample, MALDI-TOF MS shows near-quantitative conversion to the singly modified product. MS2-*p*aF19 capsids lacking the cysteine mutation showed no dye incorporation under identical conditions.

To finish synthesizing the delivery vehicle shown in Figure 1a, a 41-nucleotide DNA aptamer that targets a specific cell surface marker on Jurkat cells (strand **B**, Table 1) was chosen as the exterior targeting group. Strand **B**, previously reported as sgc8c, was isolated using a cell-SELEX process, and its binding partner was determined to be protein tyrosine kinase 7 (PTK7).[54−56] PTK7 is a transmembrane protein that is present on the surface of Jurkat T leukemia cells, as well as many other leukemia cell lines, and has been proposed as a potential biomarker for T cell acute lymphoblastic leukemia.[56] By using the oxidative coupling strategy, 20−40 copies of diethyl phenylenediamine-labeled strand **B** were attached to each capsid, as determined by SDS-PAGE and densitometry analysis (Figure 2a, lane 8). To detect the capsids in cell-binding assays, the interior was modified with AF488 chromophores as described above prior to DNA attachment.

We tested the targeting specificity of these capsids by incubating them with Jurkat cells at 37 °C for 30−60 min in culture media. Subsequent analysis using flow cytometry revealed that samples of cells exposed to MS2 capsids bearing strand **B** (11 nM in capsids) showed a significant increase in mean fluorescence intensity compared to background cellular autofluorescence, Figure 3a. For negative controls, we synthesized AF488-modified capsids with no exterior modification (AF488-MS2), as well as ones modified with a 41-nt strand of a randomized sequence (**C**, Table 1). Both control capsids did not give rise to an increase in mean fluorescence intensity, confirming the role of the specific aptamer sequence in cell binding.

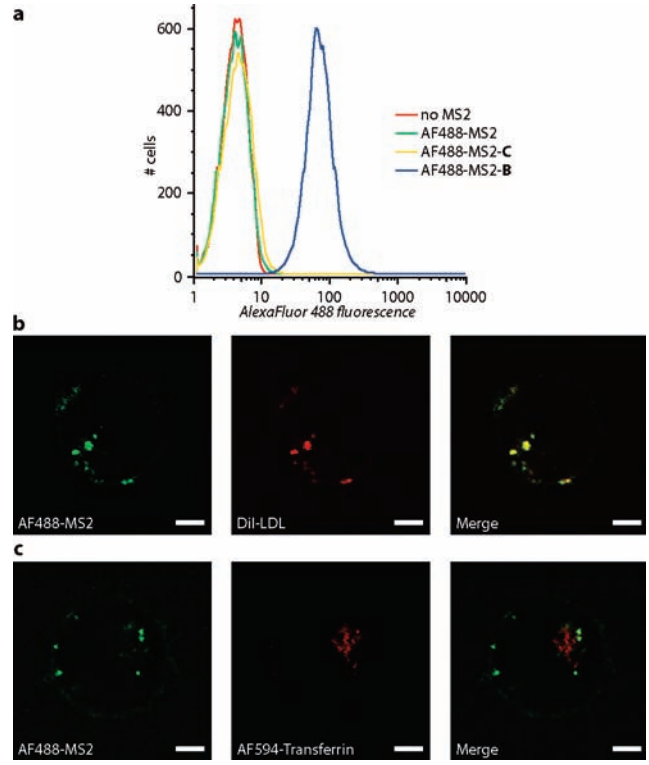

Figure 3. Cellular targeting and uptake with aptamer-labeled capsids. (a) Cell targeting was confirmed using flow cytometry. Only MS2 capsids modified with strand **B** bound to Jurkat cells (blue trace). Capsids that were unmodified on the exterior and capsids modified with strand **C** (green and yellow traces, respectively) showed only background autofluorescence (red trace). Live confocal images showed a colocalization of **B**-labeled capsids with LDL-labeled endosomes (b), but not with transferrin-labeled endosomes (c). Scale bars represent 3 μm.

Having validated the targeting of **B**-labeled capsids in flow cytometry experiments, we investigated the cellular internalization of the modified capsids with confocal microscopy. After incubation for 30−60 min at 37 °C with Jurkat cells, the presence of capsids labeled with strand **B** could be detected as brightly fluorescent dots within the cells, Figure 3b. Costaining experiments with fluorescent endocytic markers indicated that the **B**-labeled capsids colocalized with low-density lipoprotein (LDL) particles, but not transferrin. Although both transferrin and LDL are known endocytic markers, they traffic through different pathways once inside the cell. Transferrin has been shown to indicate endosomes that are directed back to the surface through the recycling pathway, whereas vesicles associated with LDL eventually traffic to lysosomes.[57] In combination with the targeting specificity of the α-PTK7 aptamer, the lysosomal fate of **B**-labeled capsids is encouraging for the

(54) Shangguan, D.; Li, Y.; Tang, Z.; Cao, Z. C.; Chen, H. W.; Mallikaratchy, P.; Sefah, K.; Yang, C. J.; Tan, W. *Proc. Natl. Acad. Sci.* **2006**, *103*, 11838–11843.
(55) Shangguan, D.; Tang, Z.; Mallikaratchy, P.; Xiao, Z.; Tan, W. *ChemBioChem* **2007**, *8*, 603–606.
(56) Shangguan, D.; Cao, Z.; Meng, L.; Mallikaratchy, P.; Sefah, K.; Wang, H.; Li, Y.; Tan, W. *J. Proteome Res.* **2008**, *7*, 2133–2139.

targeted drug delivery of acid-labile prodrugs that would be preferentially released in these compartments.

Conclusion

For any delivery vehicle composition, the attachment of unprotected biomolecular targeting agents will likely be of key importance to achieve tissue specificity. This report demonstrates the utility of a chemoselective oxidative coupling reaction for this purpose. In principle, the MS2-based vehicle described herein can now be targeted to any receptor for which a binding aptamer has been determined. For the purposes of diagnostic imaging it may not be necessary for the capsids to be internalized; however, the observed uptake is envisioned to be highly beneficial for drug delivery applications. In current experiments, we are adding anticancer drugs to these carriers, and also radionuclides and contrast agents that can be used to determine the location of cellular markers *in vivo*.

Acknowledgment. The development of the coupling reaction described in this work was supported by the NIH (R01 GM072700). Our studies of modified viral capsids as targeted imaging agents are supported by the DOD Breast Cancer Research Program (BC061995). Bryan C. Dickinson is gratefully acknowledged for lending his cell imaging expertise, and we thank Carolyn Bertozzi and her research group for cell culture assistance. The Schultz laboratory is gratefully acknowledged for providing the plasmids required to introduce *p*aF using the amber codon suppression technique.

Supporting Information Available: This material is available free of charge via the Internet at http://pubs.acs.org.

JA903857F

(57) Maxfield, F. R.; McGraw, T. E. *Nat. Rev. Mol. Cell Biol.* **2004**, *5*, 121–132.